INTERNATIONAL JOURNAL FOR NUMERICAL AND ANALYTICAL METHODS IN GEOMECHANICS, VOL. 20, 57–72 (1996)

ANALYSIS OF PILED RAFT SYSTEMS IN LAYERED SOILS

L. D. TA AND J. C. SMALL

School of Civil and Mining Engineering, University of Sydney, NSW 2006, Australia

SUMMARY

This paper presents a method of analysis for piled raft systems constructed in layered soils. The method presented takes account of the interactions of the raft, piles and soil without the cost of a full three-dimensional rigorous analysis. This is done by the use of finite layer methods for the analysis of the soil and finite element methods for the raft. Examples are provided in the paper for piled rafts constructed on layered soils, and results are presented for bending moments in the raft and loads in the piles.

KEY WORDS: piled raft systems; raft-pile-soil interaction; finite layer methods; foundations

INTRODUCTION

Piled raft foundations are commonly used to support the superstructures of bridges, buildings and heavy industrial plant. Foundation engineers need to know how the structural load is transmitted to the supporting soil and how the structural load is transferred to the piles and soil beneath. They also need to be able to compute the differential displacements and moments in the raft. Several methods have been proposed for analysing piled raft systems. Early work was carried out by Davis and Poulos.[1] Their method was based on pile to pile and pile to soil surface interactions and *vice versa*. Butterfield and Banerjee[2] analysed pile caps with compressible piles using a similar method. These methods are limited however, to rigid rafts only. Brown and Weisner[3] analysed a strip footing under a uniformly distributed load and assumed that the soil was an isotropic homogeneous elastic half-space. Later, Weisner and Brown[4] analysed a piled strip footing subject to concentrated loads. Hain and Lee[5] used the finite element method to analyse the raft, and pile group interaction factors to analyse the pile behaviour. Poulos[6] proposed the finite difference method for analysis of the raft in a piled raft system.

This paper extends the method of analysis for pile groups in layered soil which was described by Ta and Small,[7] where the soil is modelled using the finite layer method.[8,9]. The raft is modelled using the finite element method and treated as a thin elastic plate, and therefore the present method can be used to analyse a raft with any geometry and any stiffness. The soil can be considered to be an isotropic or cross-anisotropic horizontally layered material and the piles may be randomly distributed beneath the raft.

METHOD OF ANALYSIS

The raft is assumed to be a thin elastic plate and the finite element method described by Bogner *et al.*[10] is used to analyse it. The raft is divided into a number of rectangular elements (see Figure 1(a)), each element having four nodes and 16 degrees of freedom. The contact load pressures between the raft and the soil surface and between the raft and the pile heads are assumed to be uniform blocks of pressure which act over each element in the raft. Displacements at the centre of

CCC 0363–9061/96/010057–16

Received 17 March 1995
Revised 15 June 1995

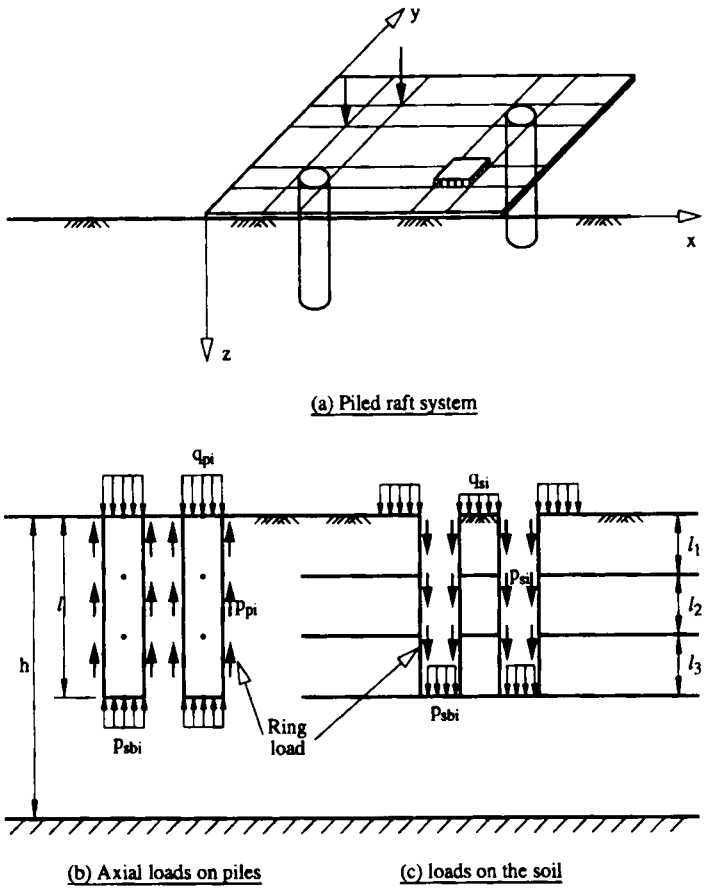

Figure 1. Forces considered to act on the piles and on the soil

each raft element can be expressed as[11]

$$\omega_r = [\mathbf{I}_r]\mathbf{Q}_r + \mathbf{a}\delta + \mathbf{b}\theta_x + \mathbf{c}\theta_y + \omega_{q0} \tag{1}$$

where $[\mathbf{I}_r]$ is the influence matrix of the pinned raft, the columns of which are the deflections at the centers of all raft elements due to a unit uniform load placed on each raft element in turn, $\mathbf{Q}_r$ the contact load pressures on the raft, ω_{q0} the vector of deflections at the centre of each raft element for the case of the pinned raft acting under the applied loads, $\mathbf{a} = (1, 1, \ldots, 1)^T$, δ the vertical translation of the raft at the pin, θ_x the x-rotation of the raft relative to the pin and θ_y the y-rotation of the raft relative to the pin, if (x_p, y_p) are the x and y co-ordinates of the pin and (x_i, y_i) are the co-ordinates of the centre of each raft element, then the lever arm vectors $\mathbf{b}$ and $\mathbf{c}$ can be written as follows:

$$\mathbf{b} = (y_1 - y_p, y_2 - y_p, \ldots, y_i - y_p, \ldots, y_n - y_p)^T$$

$$\mathbf{c} = (x_1 - x_p, x_2 - x_p, \ldots, x_i - x_p, \ldots, x_n - x_p)^T$$

The raft must be restrained from free body rotations and translations to allow the influence matrix to be assembled, and so it must be 'pinned' at one node.

The piles are assumed to have a solid circular cross-section and each pile is divided into a number of elements. The load–displacement relationship of the group of piles may be written as follows:

$$\mathbf{Q}_p + \mathbf{P}_p + \mathbf{P}_{pb} = [\mathbf{K}_p]\boldsymbol{\omega}_p \tag{2}$$

where $[\mathbf{K}_p]$ is the stiffnesses of all piles in the group, $\boldsymbol{\omega}_p$ the vector of displacements at the ends of each pile element, $\mathbf{Q}_p$ the vector of loads acting on the pile heads, $\mathbf{P}_p$ the vector of loads acting along the pile shafts and $\mathbf{P}_{pb}$ the vector of loads acting at the pile bases.

The soil is divided into a number of layers. The loads on the soil can be considered as two different types. The first is the load which is transmitted directly from the raft to the soil surface, called the contact load, $\mathbf{Q}_s$. The second is the load that is transmitted from the raft to the soil through the pile shafts, referred to as friction loads, $\mathbf{P}_s$, and the base loads, $\mathbf{P}_{sb}$. The load $\mathbf{P}_s$ is considered to be a series of ring loads along the pile shafts and $\mathbf{P}_{sb}$ is considered to be a uniform pressure at the bases. Hence, the soil displacement relationship can be written as follows:

$$\mathbf{Q}_s + \mathbf{P}_s + \mathbf{P}_{sb} = [\mathbf{K}_s]\boldsymbol{\omega}_s \tag{3}$$

where $[\mathbf{K}_s]$ is the soil stiffness matrix and $\boldsymbol{\omega}_s$ the vector of soil displacements for all the elements at the top surface, along the pile shafts and the pile bases.

Equations (2) and (3) can be combined and written as follows:

$$\mathbf{Q}_p + \mathbf{Q}_s + \mathbf{P}_p + \mathbf{P}_s + \mathbf{P}_{bp} + \mathbf{P}_{sb} = [\mathbf{K}_p]\boldsymbol{\omega}_p + [\mathbf{K}_s]\boldsymbol{\omega}_s \tag{4}$$

The equilibrium of the interaction at the pile–soil interface requires that

$$\mathbf{P}_p = -\mathbf{P}_s \tag{5}$$

and

$$\mathbf{P}_{pb} = -\mathbf{P}_{sb} \tag{6}$$

and assuming there is no slip along the shafts then the vertical displacements at the pile–soil interfaces will be the same. Equation (4) can now be written as follows:

$$\mathbf{Q}_c = [\mathbf{K}_c]\boldsymbol{\omega}_s \tag{7}$$

where

$$\mathbf{Q}_c = \mathbf{Q}_p + \mathbf{Q}_s$$

$$[\mathbf{K}_c] = [\mathbf{K}_p] + [\mathbf{K}_s]$$

In flexibility form, equation (7) may be rewritten as follows:

$$\boldsymbol{\omega}_s = [\mathbf{I}_c]\mathbf{Q}_c \tag{8}$$

where

$$[\mathbf{I}_c] = [\mathbf{K}_c]^{-1}$$

Note that $\boldsymbol{\omega}_s$ is only a function of the contact load pressures at the top surface of the soil and at the pile heads. Hence, the displacements at the raft–soil interfaces and raft–pile heads can be obtained from equation (8) by eliminating the displacements of the soil along the pile shafts and at the pile bases. Equation (8) can now be written as

$$\boldsymbol{\omega}_s^* = [\mathbf{I}_c^*]\mathbf{Q}_c \tag{9}$$

where $\boldsymbol{\omega}_s^*$ is the displacement vector at the surface interface between the raft and soil and the raft and pile heads, $[\mathbf{I}_c^*]$ is the influence matrix for the surface interface between the raft and soil and

the raft and pile heads and $\mathbf{Q}_c$ is the contact load pressure acting on the soil surface and pile heads.

The equilibrium of the contact stresses at the raft–soil interface and the raft–pile head interface requires that

$$\mathbf{Q} = \mathbf{Q}_c = -\mathbf{Q}_r \tag{10}$$

and the compatibility of the displacements between the raft and the soil surface and pile heads requires

$$\boldsymbol{\omega}_r = \boldsymbol{\omega}_s^* \tag{11}$$

Combining equations (1) and (9), the following equation is obtained:

$$([\mathbf{I}_c^*] + [\mathbf{I}_r])\mathbf{Q} - \mathbf{a}\delta - \mathbf{b}\theta_x - \mathbf{c}\theta_y = \boldsymbol{\omega}_{q0} \tag{12}$$

Three further equilibrium equations are needed before the solution can be obtained.
the vertical equilibrium equation:

$$\mathbf{a}^T\mathbf{Q} = Q_{Tot} \tag{13}$$

equilibrium of moments about the x-axis:

$$\mathbf{b}^T\mathbf{Q} = M_{apx} \tag{14}$$

equilibrium of moments about the y-axis:

$$\mathbf{c}^T\mathbf{Q} = M_{apy} \tag{15}$$

where Q_{Tot} is the total applied load on the raft, M_{apx} the total applied moment in the x-direction and M_{apy} the total applied moment in the y-direction.

A combination of equations (12)–(15) results in

$$\begin{bmatrix} [\mathbf{I}_c^*] + [\mathbf{I}_r] & -\mathbf{a} & -\mathbf{b} & -\mathbf{c} \\ -\mathbf{a}^T & 0 & 0 & 0 \\ -\mathbf{b}^T & 0 & 0 & 0 \\ -\mathbf{c}^T & 0 & 0 & 0 \end{bmatrix} \begin{bmatrix} \mathbf{Q} \\ \delta \\ \theta_x \\ \theta_y \end{bmatrix} = \begin{bmatrix} \boldsymbol{\omega}_{q0} \\ -Q_{Tot} \\ -M_{apx} \\ -M_{apy} \end{bmatrix} \tag{16}$$

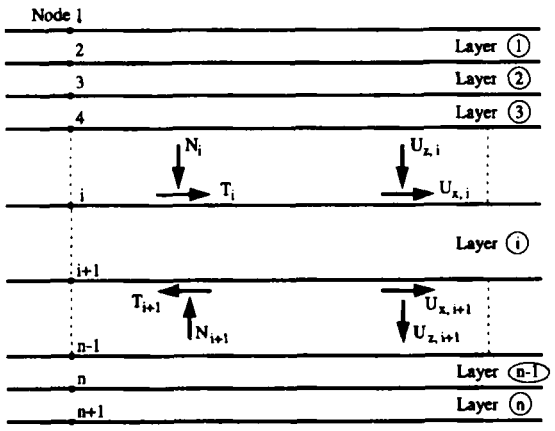

Figure 2. Layered soil system

From this equation, we can find the translation δ, the rigid body x and y rotations θ_x and θ_y and contact pressures **Q** on the raft. The displacements of the soil along the shafts and bases of the piles and at the surface of the soil can be found from equation (8). The pile loads (on the head, along the shaft and the base) can be found from equation (2).

FINITE LAYER METHOD

The finite layer method can be used to solve problems where the soil is made up of a number of horizontal layers, as shown in Figure 2. Soil layers can consist of isotropic or cross-isotropic materials. In the finite layer method, stresses and displacements are often expressed in terms of their Fourier or Hankel transforms. The relationship of the stress transforms and the

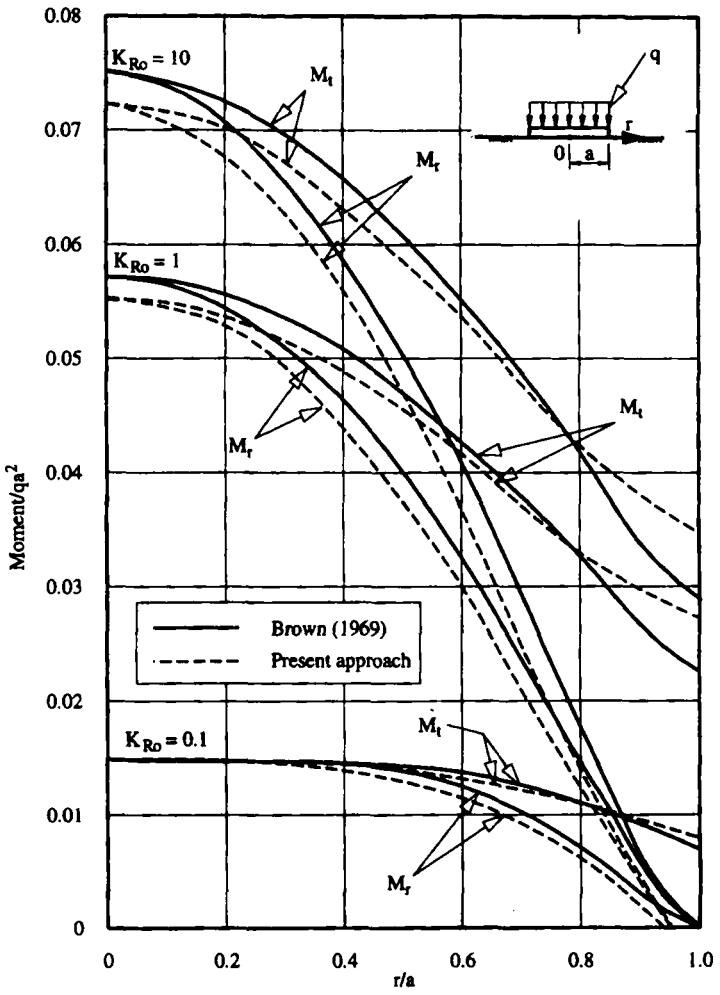

Figure 3. Bending moment distributions along the radius of the circular raft

displacement transforms of element i in Figure 2 can be written as follows:

$$\begin{bmatrix} N_i \\ T_i \\ -N_{i+1} \\ -T_{i+1} \end{bmatrix} = \begin{bmatrix} k_{11} & k_{12} & k_{13} & k_{14} \\ k_{21} & k_{22} & k_{23} & k_{24} \\ k_{31} & k_{32} & k_{33} & k_{34} \\ k_{41} & k_{42} & k_{43} & k_{44} \end{bmatrix} \begin{bmatrix} U_{z,i} \\ U_{x,i} \\ U_{z,i+1} \\ U_{x,i+1} \end{bmatrix} \tag{17}$$

where N is the normal stress transform, T is the shear stress transform. U_z and U_x are displacement transforms in the vertical and horizontal directions, respectively.

Using vector notation, equation (17) can be written as

$$\mathbf{F}_i = [k_i]\mathbf{U}_i \tag{18}$$

The total stiffness matrix $[\mathbf{K}]$ for n layers of soil can be constructed from the sum of the n layer element stiffness matrices $[k_i]$. As the total stiffness matrix is assembled, all transformed inter-layer stresses will cancel out. For example, if only a vertical load is applied at node i then

$$\mathbf{F} = [\mathbf{K}]\mathbf{U} \tag{19}$$

where

$\mathbf{F} = (0, 0, \ldots, N_i, 0, \ldots, N_{n+1}, T_{n+1})$ vector of stress transforms

$\mathbf{U} = (U_{z,1}, U_{x,1}, U_{z,2}, U_{x,2}, \ldots, U_{z,n+1}, U_{x,n+1})$ vector of displacement transforms

$[\mathbf{K}] = \sum [k_i]$

The unknown stress transforms N_{n+1} and T_{n+1} at the base can be eliminated by applying a displacement boundary condition, i.e. $U_{z,n+1} = U_{x,n+1} = 0$.

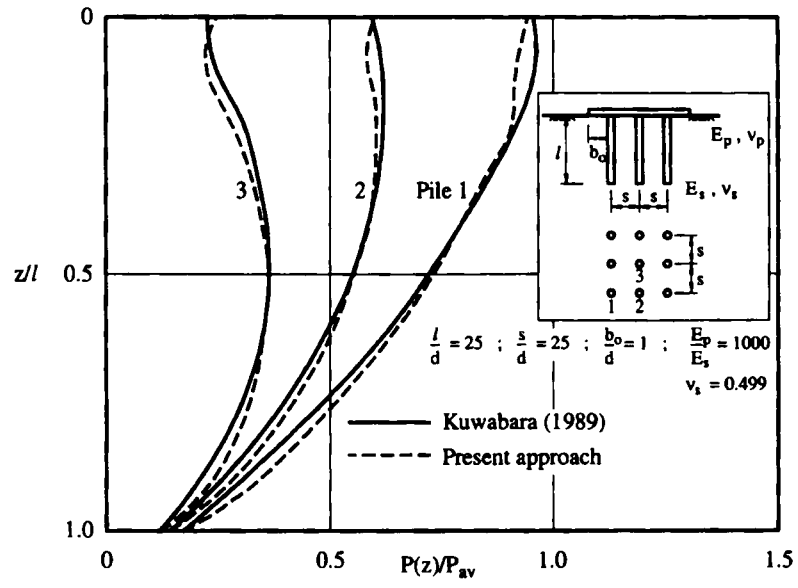

Figure 4. Vertical load distributions along the pile shafts

Circular and ring loads

Ring loads and a uniform circular loading are assumed to be applied to the shaft and base of the pile, respectively. The displacements in the soil due to shaft and base loads for each pile are used in establishing the stiffness matrix of equation (3). Stresses and displacements of a point anywhere in the soil can be expressed using an inversion of the Hankel transforms.

$$\sigma_{zz} = \int_0^\infty \alpha S_{zz} J_0(\alpha r)\, d\alpha \tag{20}$$

$$u_z = \int_0^\infty \alpha U_z J_0(\alpha r)\, d\alpha \tag{21}$$

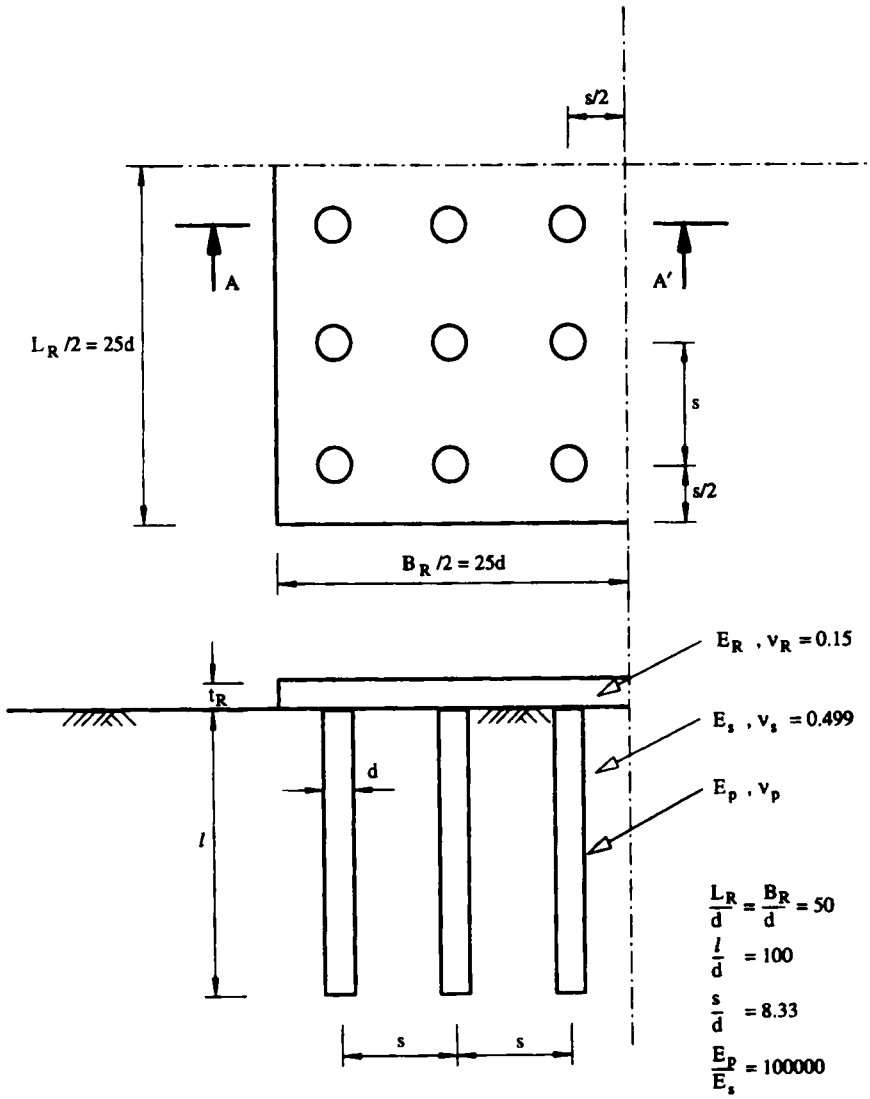

Figure 5. Details of raft, piles and soil

Stress transforms are obtained using a Hankel transform and can be written as follows:

$$S_{zz} = \int_0^\infty r\sigma_{zz} J_0(\alpha r)\, dr \tag{22}$$

If q is a uniform distributed load on a circle with radius R then the stress transform S_{zz} becomes

$$N = S_{zz} = \frac{qR}{\alpha} J_1(\alpha R) \tag{23}$$

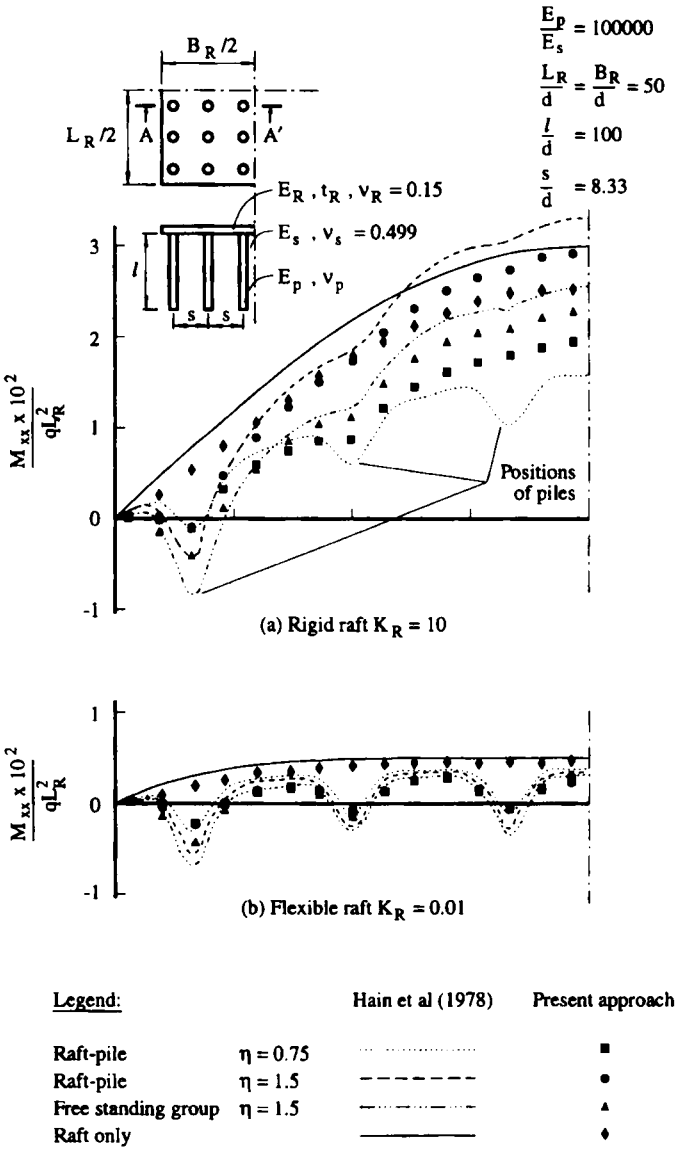

Figure 6. Bending moment per unit length (M_{xx}) distributed along section A–A': (a) Rigid raft $K_R = 10$; (b) flexible raft $K_R = 0.01$

and if Q is a ring load with radius R (Q is the total load) then

$$N = S_{zz} = \frac{Q}{2\pi} J_0(\alpha R) \tag{24}$$

Rectangular load

For rectangular loading, the stresses and displacements of a point in the soil field can be expressed as an inverse Fourier integral.[9] This can be used to compute deflections at any position in the soil due to contact stresses applied over a rectangular region on the soil surface and is used in obtaining the stiffness matrix of equation (3). For example,

$$\sigma_{zz} = \int_{-\infty}^{+\infty} \int_{-\infty}^{+\infty} S_{zz} \cos(\alpha x) \cos(\beta y) \, d\alpha \, d\beta \tag{25}$$

$$u_z = \int_{-\infty}^{+\infty} \int_{-\infty}^{+\infty} U_z \cos(\alpha x) \cos(\beta y) \, d\alpha \, d\beta \tag{26}$$

To obtain the stress transform we apply a double Fourier integral, e.g.

$$S_{zz} = \frac{1}{4\pi^2} \int_{-\infty}^{+\infty} \int_{-\infty}^{+\infty} \sigma_{zz} \cos(\alpha x) \cos(\beta y) \, dx \, dy \tag{27}$$

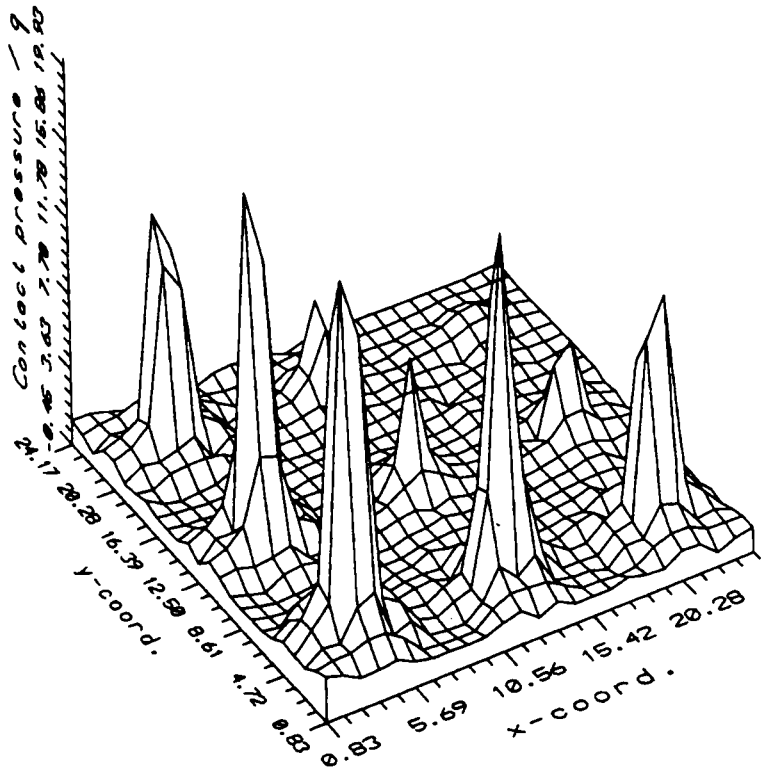

Figure 7. Contact load pressure on the raft for $K_R = 10$ and $\eta = 1.5$

If q is a uniform distributed load on a rectangular area with width of $2a$ and length of $2b$ then the transform of vertical stress becomes

$$N = S_{zz} = \frac{q}{\pi^2} \frac{\sin(\alpha a)\sin(\beta b)}{\alpha\beta} \tag{28}$$

Soil stiffness matrix

The soil influence matrix can be calculated as follows. Apply a unit load (ring load along the pile shaft; uniform circular pressure at the pile base; a uniform block pressure at the soil surface) on each soil element in turn and calculate the displacement of all elements in the soil. This will form a column of the soil influence matrix. The soil stiffness matrix can be calculated by inversion of the soil influence matrix.

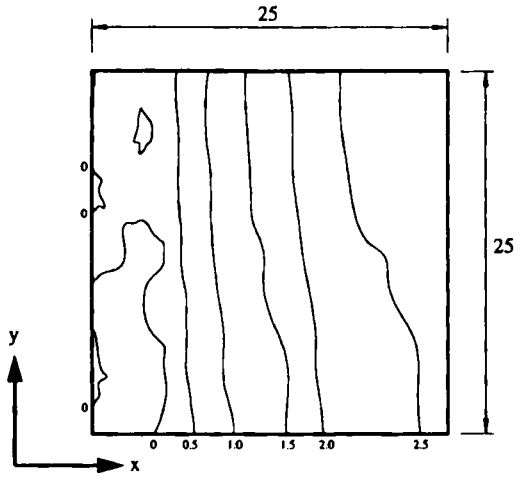

Figure 8. Contours of the bending moment $M_{xx}/qL_R^2 \times 10^2$ for $K_R = 10$ and $\eta = 1.5$

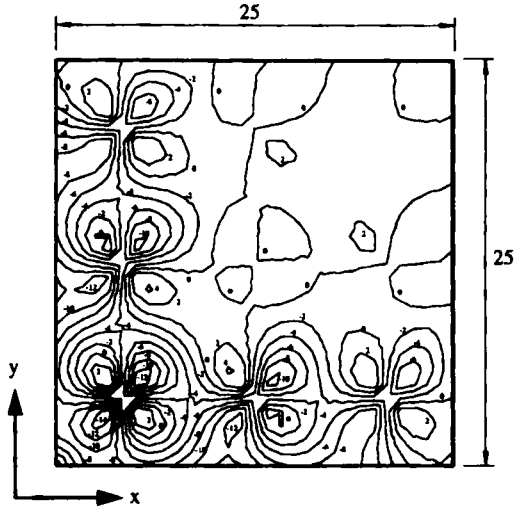

Figure 9. Contours of the twisting moment $M_{xy}/qL_R^2 \times 10^4$ for $K_R = 10$ and $\eta = 1.5$

Large problems

This method requires storage of fairly large fully populated matrices, e.g. $[\mathbf{K}_c]$ (Equation (7)). The program used to compute results for this paper allows for up to 1200 raft and pile elements altogether. However, storage and time requirements increase rapidly with the size of the problem. The time required to solve large problems can take several hours on a personal computer if the

Table I. Material properties of soils

	E_H/E_V	G_V/E_V	ν_{HH}	ν_{HV}	ν_{VH}	E_{V1}/E_{V2}
Material 1	2	0.45	0.25	0.35	0.175	0.2
Material 2	3	0.5	0.1	0.9	0.3	—

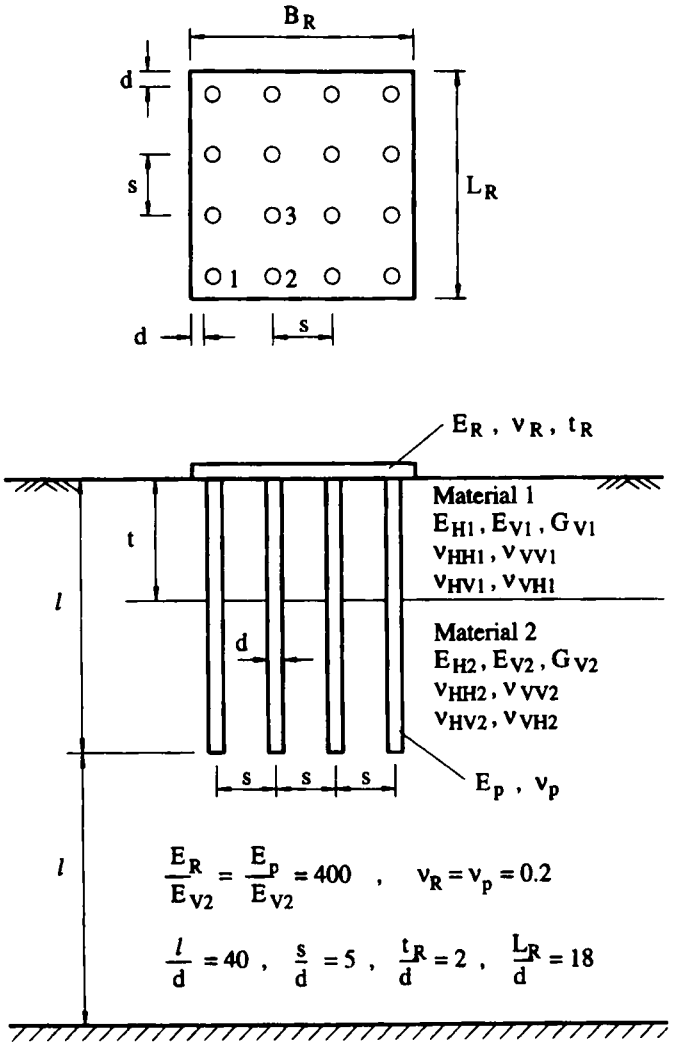

Figure 10. Details of raft, piles and cross-anisotropic soils

interaction of all ring, circular and rectangular loads are computed directly. However, computation time can be reduced dramatically using a technique which will be discussed in a future paper.

RESULTS

In the following examples which demonstrate the use of the foregoing theory, all the piles were assumed to be identical and have a circular cross-section. Each pile was divided into 10 equal elements.

Brown[12] has presented solutions for uniformly loaded unpiled circular rafts resting on deep elastic homogeneous soils. Figure 3 shows the plots of tangential and radial moments along the radius for three different relative raft stiffnesses $K_{RO} = 0.1$, 1 and 10 ($K_{RO} = [E_R(1 - \nu_s^2)/E_s](t_R/a)^3$ where E_R is Young's modulus of the raft, E_s and ν_s are Young's modulus and Poisson's ratio of the soil respectively, t_R is the raft thickness and a is the radius of the raft). The results of the present method are also shown in Figure 3 where it may be seen that they are in reasonably close agreement with Brown's solutions. The difference in the solutions is due to the fact that in the analytic solution, the contact stresses are infinite at the edge of the raft, whereas in the solution presented here, they are finite. Hence for the raft, moments may be a little less than predicted by rigorous elastic theory, but are not likely to be seriously in error as in reality, the stresses cannot become infinite at the edge of the raft.

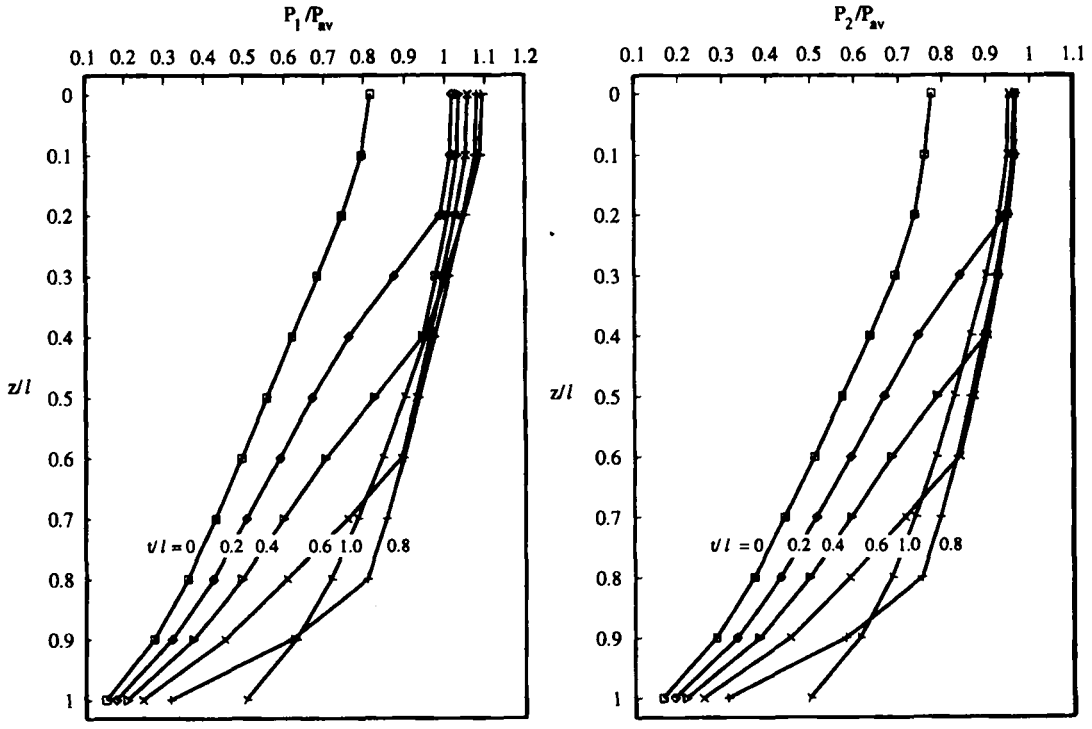

(a) Pile 1 (b) Pile 2

Figure 11. Loads in pile shaft for various ratios of upper soil layer thickness to pile length t/l: (a) pile 1; (b) pile 2; (c) pile 3

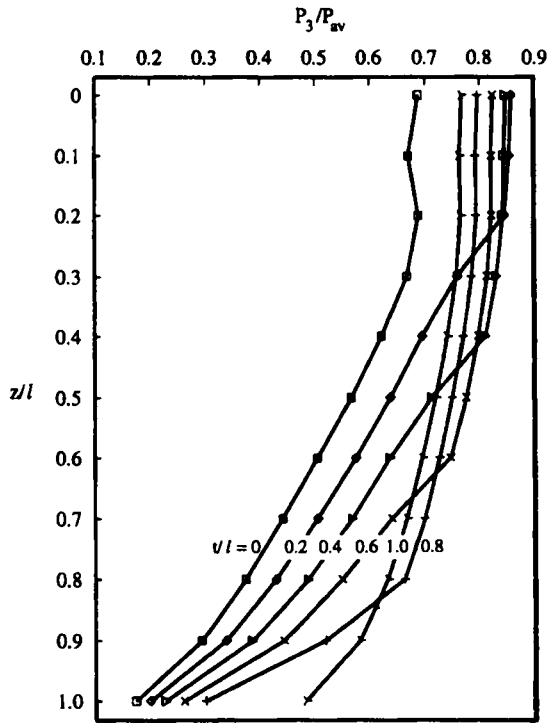

(c) Pile 3

Figure 11. (Continued)

Kuwabara[12] analysed the behaviour of a piled raft system made up of 9 piles. The raft was assumed to be perfectly rigid and was loaded by a uniform load with a total load of P_{tot}. The soil was assumed to be a homogeneous isotropic elastic half-space. Figure 4 shows the relative load ratio $P_i(z)/P_{av}$ distributed along the pile shafts where $P_i(z)$ is the vertical load on pile i at depth z and P_{av} is the average pile head load ($P_{av} = P_{tot}/N$ where N is the number of piles). Figure 4 also shows that the Kuwabara solutions predict slightly smaller loads along the lower sections of the pile shaft and slightly higher loads at the top of the shaft than the present method. Overall, the loads predicted in the piles by both methods can be seen to be reasonably close.

Hain and Lee[5] have presented an analysis of flexible raft–pile systems. Their method allows for the limiting of the ultimate axial load capacity on the pile heads. They introduced a load cut-off parameter, η, as follows:

$$\eta = \frac{NP_{ult}}{qL_R B_R} \tag{29}$$

where P_{ult} is the ultimate load capacity of each pile, q is uniform distributed load on the raft, L_R is the length of the raft and B_R is the breadth. The relative stiffness between the raft and supporting soil is defined as follows:

$$K_R = \frac{4E_R t_R^3 B_R(1 - \nu_s^2)}{3\pi E_s L_R^4} \tag{30}$$

and the relative stiffness between pile and soil is defined as $K_p = E_p/E_s$, where E_p is the Young's modulus of the pile. All other parameters have been defined previously.

Hain and Lee[5] analysed a piled raft with a group of 6 x 6 piles beneath one-quarter of the raft as shown in Figure 5. Moments along section A–A′ are plotted in Figures 6(a) and (b), where the raft can be either clear of the ground (free-standing group) or in contact with the ground surface (raft–pile).

For the flexible raft ($K_R = 0.01$), the computed moments per unit length are slightly smaller than those of Hain and Lee but it may be seen from Figure 6(b) that they show the same trend in that there is a local reduction in moment where the raft passes over the pile head.

For the stiffer raft ($K_R = 10$), the computed moments are smaller than the Hain and Lee predictions (Figure 6(a)) for both a free-standing raft and a raft in contact with the ground ($\eta = 1.5$). However, where $\eta = 0.75$ (cap on ground) the computed results are very different to the Hain and Lee results with the moments being higher and the local reduction in moment in the vicinity of the pile head not as great as in the Hain and Lee prediction.

Results are shown on the plots for the raft only (full lines) and the values computed by the present method compared. It can be seen that the Hain and Lee solutions overestimate the values of bending moments as calculated by the present method. A comparison with Brown's[12] solution, treating the square raft as a circular one of equal area, also showed that the Hain and Lee results overestimated the bending moments.

The contact load pressure acting under the raft is plotted in Figure 7 for the case of a rigid piled raft ($K_R = 10$ and $\eta = 1.5$). From Figure 7, it can be seen that the outer piles carry more load than the inner ones. The contours of the bending moments per unit length, M_{xx} and M_{xy}, in the raft are also shown in Figures 8 and 9, respectively.

Having tested the computer program against existing solutions, the method was applied to some original problems. Figure 10 shows the geometry of a uniformly loaded square raft underpinned by a 4 x 4 group of piles which is embedded in a cross-anisotropic material. The soil parameters are shown in Table I. Figures 11(a)–(c) show the effect of the relative thickness t/l of

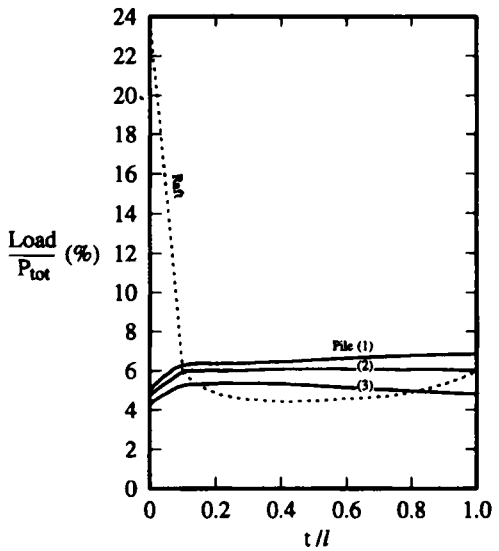

Figure 12. Percentage of loads carried on each pile and on the raft

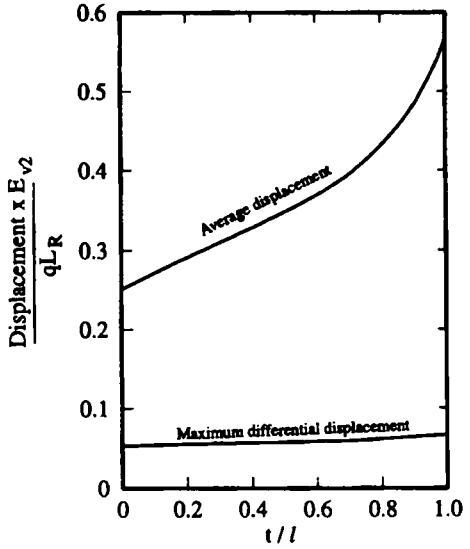

Figure 13. Effect of ratio t/l on average vertical displacement and maximum differential displacement in the raft

the top layer to the load distribution along the pile shafts. The results show that the distributed load at the lower parts of the pile shafts are very sensitive to the ratio t/l. Figure 12 shows the percentage of loads carried on the raft and on each pile head for various values of the t/l ratio. It can be seen that when there is no upper layer ($t = 0$) the raft carries a large percentage of the load. Figure 13 shows the effect of the ratio t/l on average vertical displacement and maximum differential displacement in the raft. This plot shows that the average deflection of the raft becomes larger as the upper (less stiff) layer of soil becomes thicker as do the differential (corner to centre) displacements. The average deflection is affected more by the increase in the upper layer thickness than is the differential deflection in this example.

CONCLUSIONS

This paper presents an effective method for the analysis of piled raft systems constructed in layered soils. The method combines both the finite element method for rafts and the finite layer method for soil–pile groups. Solutions can be obtained for most of the quantities required by designers such as differential settlements and moments in the raft, loads in the piles and overall deflections in the raft. This method can also be used for layered soils and the soil can be homogeneous, non-homogeneous or have cross-anisotropic properties.

The examples given show that the method can be used successfully for the analysis of piled raft groups in layered soils, and that the load distributions along the shafts of piles in layered soils are affected by the relative thickness and stiffness of soil layers.

REFERENCES

1. E. H. Davis, and H. G. Poulos, 'The analysis of pile raft systems', *Australian Geomech. J.*, **G2**, 21–27 (1972).
2. R. Butterfield, and P. K. Banerjee, 'The problem of pile group-pile cap interaction', *Géotechnique*, **21**, 135–142 (1971).
3. P. T. Brown, and T. J. Wiesner, 'The behaviour of uniformly loaded piled strip footings', *Soils Found.*, **15**, 13–21 (1975).

4. T. J. Wiesner, and P. T. Brown, 'Behaviour of piled strip footings subject to concentrated loads', *Australian Geomech. J.*, **G6,** 1–5 (1976).
5. S. J. Hain and I. K. Lee, 'The analysis of flexible raft-pile systems', *Géotechnique*, **28,** 65–83 (1978).
6. H. G. Poulos, 'An approximate numerical analysis of pile–raft interaction', *Int. j. numer analyt. methods geomechs.*, **18,** 73–92 (1994).
7. L. D. Ta, and J. C. Small 'Finite layer analysis of pile groups in layered soils', *Int. Symp. on Numerical Models in Geomechanics*, Davos, Switzerland, 1995, accepted.
8. J. C. Small and J. R. Booker, 'Finite layer analysis of layered elastic materials using a fexibility approach. Part 1—strip loadings', *Int. j. numer. methods eng.*, **20,** 1025–1037 (1984).
9. J. C. Small, and J. R. Booker, 'Finite layer analysis of layered elastic materials using a flexibility approach. Part 2—circular and rectangular loadings', *Int. j. numer. methods eng.* **23,** 959–978 (1986).
10. F. K. Bogner, R. L. Fox, and L. A. Schmit, 'The generation of interelement-compatible stiffness and mass matrices by the use of interpolation formulas', *Proc. Conf. Matrix Meth. Struct. Mech.*, Wright-Patterson AFB, OH (AFFDL-TR-66-88), 1965, 397–443 (1965).
11. B. Q. Zhang and J. C. Small, 'Analysis of rafts on foundations of variable stiffness', *Proc. 7th Int. Conf. on Computer Meth. and Advances in Geomechs.*, Cairns, 6–10 May, Vol. 2, 1991, 1103–1108.
12. P. T. Brown, 'Numerical analyses of uniformly loaded circular rafts on deep elastic foundations', *Géotechnique*, **19,** 399–404 (1969).
13. F. Kuwabara, 'An elastic analysis for piled raft foundations in a homogeneous soil', *Soils Found.*, **29,** 82–92 (1989).